Meteorol Atmos Phys (2009)
DOI 10.1007/s00703-008-0338-z
Printed in The Netherlands

Meteorology and Atmospheric Physics

GAME/CNRM (METEO-FRANCE/CNRS), Toulouse, France

Idealized mesoscale numerical study of Mediterranean heavy precipitating convective systems

R. Bresson, D. Ricard, V. Ducrocq

With 8 Figures

Received 26 October 2007; Accepted 12 August 2008
Published online 5 March 2009

Summary

The western Mediterranean mountainous areas are prone to heavy precipitating events during the fall season. The ingredients that favour these systems are well known but it is still difficult to understand why a precipitating system can become paroxysmal or to forecast the accurate location of the system. To investigate these predictability issues, an idealized framework to simulate quasi-stationary mesoscale convective systems is set up and serves as a basis for studying the sensitivity of the location and intensity of precipitating systems to the characteristics of the low-level upstream flow over the Mediterranean Sea. High resolution simulations are performed with the non-hydrostatic MESO-NH model for an idealized moist unstable flow but using the real topography. Low-level humidity distribution, convective available potential energy and speed of the flow are varied. It is found that various lifting mechanisms are involved to explain the specific location (orographic lifting, cold pool dynamics, low-level convergence due to deflection of the flow by the Alps). When the speed of the upstream flow is increased (decreased) compared to the CTRL run, the area of precipitation moves downstream (upstream). When the mixing ratio of the environment outside of the jet is less (more) than the CRTL run, the system is located more upstream (downstream). When the instability of the upstream flow is increased (decreased) compared to the CTRL run, the convective system moves upstream (downstream). The cold pool strength increases with slower flow and/or more instability. The maximum of rainfall is obtained when the convective system is over the relief with a strong low-level flow or a weak CAPE. The area covered by heavy precipitation is maximum when CAPE is high or low-level flow is strong.

Correspondence: Didier Ricard, GMME/MICADO, GAME/CNRM (Meteo-France/CNRS), av. G. Coriolis 42, 31057 Toulouse, France (E-mail: didier.ricard@meteo.fr)

1. Introduction

The western Mediterranean mountainous areas are prone to heavy precipitating events during the fall season. Most of them are associated with quasi-stationary frontal or mesoscale convective systems. In particular the French region Cévennes-Vivarais (southeast of the Massif Central) experiences frequent intense events, which can lead to flash-flood disasters like the one recorded in September 2002 over the Gard region with about 700 mm recorded in 24 hours (Delrieu et al. 2005). Several studies (Ricard 2005; Davolio et al. 2006; Ducrocq et al. 2008; Nuissier et al. 2008) have focused on heavy precipitating systems over the southeastern of the Massif Central on a case study basis and have highlighted various contributions of the relief, either due to the Massif Central itself or upstream of the Massif Central through neighbouring mountain ranges (the Alps, the Pyrenees): orographic lifting, steering flow, interaction with cold pool . . . In most of the cases a southerly to southeasterly flow transports heat and moisture

supplied by a warm sea during late summer and autumn and impinges the southeastern flank of the Massif Central. Moreover, deflection by the Alps and the Pyrenees creates upwind offshore low-level convergence that can release convective instability. In the case of a quasi-stationary convective system, cells are repeatedly triggered at the same location by local forcing (convergence lines, orographic lifting...), which compensates the northward propagation of mature cells (Ricard 2005). A cold pool can also appear under favourable conditions. In that case, the triggering of new convective cells is forced at the leading edge of the cold pool, which can be blocked in the valleys (Ducrocq et al. 2008).

The ingredients that favour heavy precipitation systems are well known (Lin et al. 2001) but it is still difficult to understand why a precipitating system can become paroxysmal or to forecast the accurate location of the system. To go one step further in these predictability issues, an idealized framework to simulate quasi-stationary mesoscale convective systems is set up here and serves as a basis for studying the sensitivity of the location and intensity of precipitating systems regarding the characteristics of the low-level flow over the Mediterranean Sea.

2. Numerical set up

High resolution simulations are performed with the non-hydrostatic MESO-NH model (Lafore et al. 1998) for an idealized moist unstable flow but using the real topography as in Gheusi and Stein (2003). The domain at 2.5 km horizontal resolution is centred over the Mediterranean coast of southeastern France. Initial and boundary conditions for temperature and humidity are derived from the Nîmes sounding of the extreme Gard flood case at 12 UTC, 8 September 2002 (Fig. 1a). Surface fields (SST, soil temperature and water content) are initialized from the ARPEGE analysis (12 UTC, 8 September). A unidirectional south-southeasterly wind is imposed through the whole depth of the atmosphere in the initial and boundary conditions. In order to represent the low-level south-southeasterly jet that prevails during heavy precipitation events over this region, strongest winds U (U = 15 m/s for the control experiment) are focused in

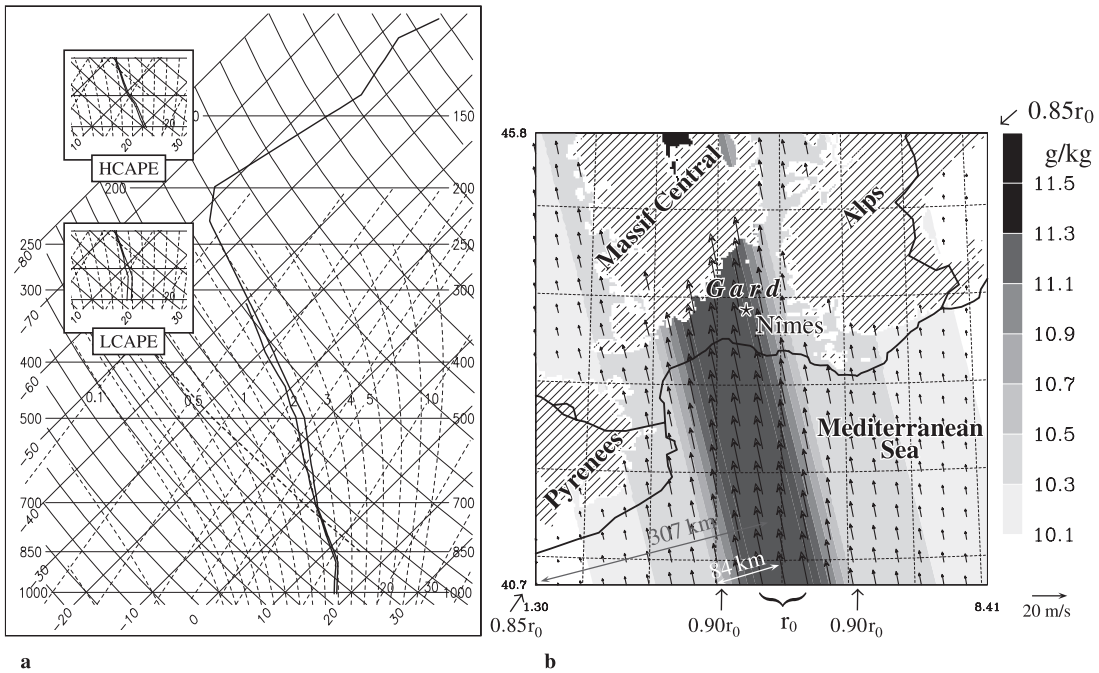

Fig. 1a. Sounding of Nîmes at 12 UTC, 8 September 2002 (Gard flood case), low-level modifications of sounding for simulations LCAPE and HCAPE are also displayed. (**b**) Initial mixing ratio of vapour at 500 m (grey scale, g/kg) and 500-m ASL wind vectors (black arrows, m/s) for simulation CTRL. The relief above 500 m is represented by the hatched areas. r_0 is equal to 11.7 g/kg inside the jet at 500 m, the distances from the centre of the jet for which the mixing ratio is reduced to $0.90r_0$ and to $0.85r_0$ are also indicated

Table 1. Characteristics of initial conditions for the different experiments. Maximum (mm), spatially integrated amount (km^3) and precipitating area (km^2) for 24-h accumulated rainfall considering two thresholds (1 and 200 mm) and area of the cold pools (km^2) considering two temperature thresholds (292 and 294.5 K) after 48 h for the different experiments

Experiments		**CTRL**	**UNIHU**	**LOWHU**	**WIN10**	**WIN20**	**LCAPE**	**HCAPE**
Initial conditions								
Humidity distribution		$\alpha = 0.9$ $\beta = 0.85$	$\alpha = 1$ $\beta = 1$ uniform	$\alpha = 0.75$ $\beta = 0.60$	as CTRL	as CTRL	as CTRL	as CTRL
U (m/s)		15	15	15	10	20	15	15
Initial CAPE (J/kg)		400	400	400	400	400	190	1760
Precipitating system characteristics								
Maximum accumulated rainfall (mm)		615	460	897	541	984	998	837
Spatially integrated amount	> 1 mm	4.50	3.10	3.29	2.93	5.55	3.78	6.24
of precipitation (km^3)	> 200 mm	2.93	0.62	2.22	1.20	3.71	2.45	3.89
Precipitating area (km^2)	> 1 mm	54259	77403	36098	59800	47681	45176	67525
	> 200 mm	8104	2269	4729	4159	9251	5599	10472
Area of cold pool (km^2)	< 292 K	587	0	461	6128	0	0	8542
	< 294.5 K	8202	1446	19100	18109	98	870	41426

a 100 km-wide band. The band has a southeast-northwest orientation so that the jet points towards the southeast flank of the Massif Central. Below 3000 m, on each side of this band, the wind decreases sharply up to zero on the southwest and northeast edges of the domain (Fig. 1b). Above 3000 m, the winds increase linearly up to 5000 m to become uniform and of intensity U. Thus for the initial conditions there is a uniform jet in the middle of the channel and a vertically sheared profile at the sides. However, during the simulation, the surface roughness modifies the wind profile in the planetary boundary layer. Assuming a unidirectional wind may exclude some effects on the organization of the convection. It is indeed recognised that rotation of winds with altitude can favour the decoupling of updrafts and precipitation and therefore the maintenance of the convective system. Moisture is also concentrated within the jet, so that the mixing ratio of water vapour is set to a value r_0 (Z) within the jet, then it linearly decreases out of the jet up to αr_0 and βr_0 as indicated in Fig. 1b ($\alpha = 0.90$, $\beta = 0.85$ and r_0 ($Z = 500$ m) $= 11.7$ g/kg for the control experiment). The temperature field is horizontally homogeneous. Then, from this control simulation, low-level humidity distribution, convective available potential energy and speed of the flow are varied (Table 1) in order to investigate the sensitivity of the location and intensity of the precipitating systems to the characteristics of the low-level flow.

3. Results

3.1 Control simulation

The CTRL simulation succeeds in simulating a quasi-stationary back-building mesoscale convective system (Schumacher and Johnson 2005) within a few hours. This is illustrated by Fig. 2a–c which shows the 24-h accumulated precipitation for three successive 24-h periods and the low-level conditions at the end of each 24-h period. After a transition period at the beginning of the simulation which lasts about 12 hours, the precipitation patterns become quite steady as confirmed by very similar patterns obtained for the two last periods (Fig. 2b, c). Table 1 lists some quantitative attributes of the 24-h accumulated precipitation fields for each simulation after 48 hours of simulation; these attributes are the maximum of the 24-h accumulated precipitation as well the area and the spatially integrated amount of precipitation for the surface collecting more than 1 mm and 200 mm in 24 h, respectively. For CTRL, the precipitation covers a vast area (54259 km^2, Table 1) that spreads from the Sea to the Massif Central (Fig. 2b). Large amounts of accumulated precipitation are simulated with a maximum value of the same order as those recorded for extreme heavy precipitation events observed over that region (Table 1). Indeed, the 24-h accumulated precipitation maximum in CTRL (615 mm) is very similar to the maximum observed during the 2002 Gard flood case (about

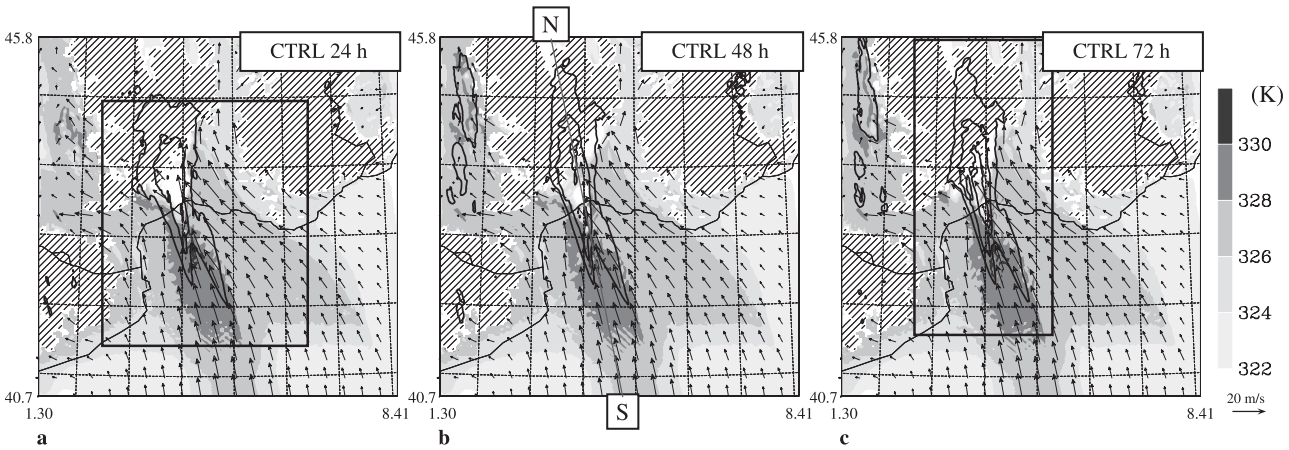

Fig. 2. Equivalent potential temperature at 500 m (grey scale, K), 500-m ASL wind vectors (black arrows, m/s) and 24-h accumulated precipitation (black lines, 50, 100, 250 and 500 mm) for simulation CTRL after 24 h (**a**) and 48 h (**b**) and 72 h (**c**). The relief above 500 m is represented by the hatched areas. Black boxes show the subdomains displayed in Fig. 3 or used for Fig. 7. Line S–N indicates the position of the vertical cross-sections shown in Fig. 5

690 mm). As in the Gard 2002 event, the precipitating system affects the plain area, although the real system extended more eastward over the Gard area (Nuissier et al. 2008). A cold pool, delineated by virtual potential temperature less than 294 K in Fig. 3g, forms under the system leaning against the southeastern flank of the Massif Central and spreading southward over the Sea. This cold pool is generated underneath the convective system by evaporation of the falling precipitation in the sub-saturated low levels. The cold pool dynamics is similar to that of a classic density current, with the environmental air being forced up and over its leading edge. As the moist and unstable low-level jet impinges the cold pool, it induces updrafts that trigger new convective cells preferably on the leading edge of the cold pool facing the low-level jet. It complies with the cold-pool-shear interaction theory originally introduced by Rotunno et al. (1988). According to this theory, the circulation associated with the vertical shear counteracts some of the circulation associated with the cold pool on the down-shear side, producing deeper lifting there. Deflection of the flow by the Alps also reinforces the low-level convergence and triggering of new convective cells. Indeed, a part of the flow reaching the Alps is deviated westward under the effects of the Coriolis force. Weaker humidity outside of the moist jet favours the leftward deflection of the unsaturated air flow that is blocked by the Alps as shown in Rotunno and Ferretti (2001). Streamlines in Fig. 4a clearly evidence this cross-barrier flow (labelled A in Fig. 4a) and the induced low-level convergence that build up from the beginning of the simulation. Later during the simulation (Fig. 4d), the cold pool dynamics modifies the low-level circulation, with the maximum of low-level convergence at the leading edge of the cold pool facing the incident flow. The cross-barrier flow contributes to reinforce this low-level convergence.

Backward trajectories for parcels taken within the anvil of the convective system (at 12 km height) show that these parcels originate from the low-level moist jet (Fig. 5); these parcels are lifted over the cold pool and then are carried up to the tropopause by strong convective updrafts. As for parcels taken within the cold pool, they originate from drier mid-layer and then are carried down by downdrafts (see Fig. 3g) where heavy precipitation occurs. Entrainment of this drier air helps the evaporation of falling rainwater that generates cooling and convective downdrafts beneath the cloudy system. Figure 5 shows that there is a crossover zone around 2000–3000 m where updrafts and downdrafts cross.

3.2 Effect of the low-level moisture

Then, by modifying the mixing ratio of water vapour, the low-level moisture outside the jet has been either decreased (simulation LOWHU, Table 1) or increased to reach a uniform moisture distribution (simulation UNIHU) for the initial and boundary conditions.

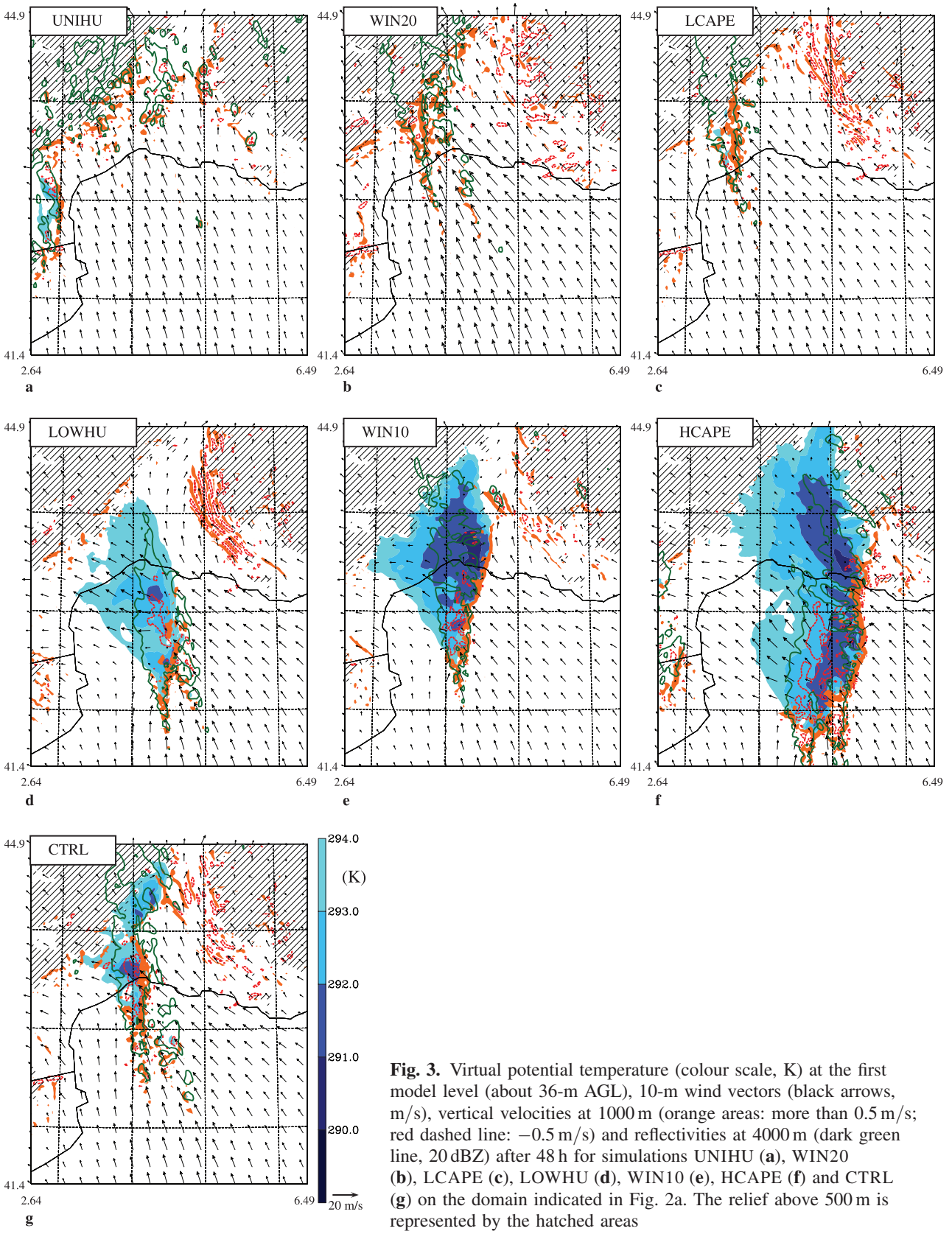

Fig. 3. Virtual potential temperature (colour scale, K) at the first model level (about 36-m AGL), 10-m wind vectors (black arrows, m/s), vertical velocities at 1000 m (orange areas: more than 0.5 m/s; red dashed line: −0.5 m/s) and reflectivities at 4000 m (dark green line, 20 dBZ) after 48 h for simulations UNIHU (**a**), WIN20 (**b**), LCAPE (**c**), LOWHU (**d**), WIN10 (**e**), HCAPE (**f**) and CTRL (**g**) on the domain indicated in Fig. 2a. The relief above 500 m is represented by the hatched areas

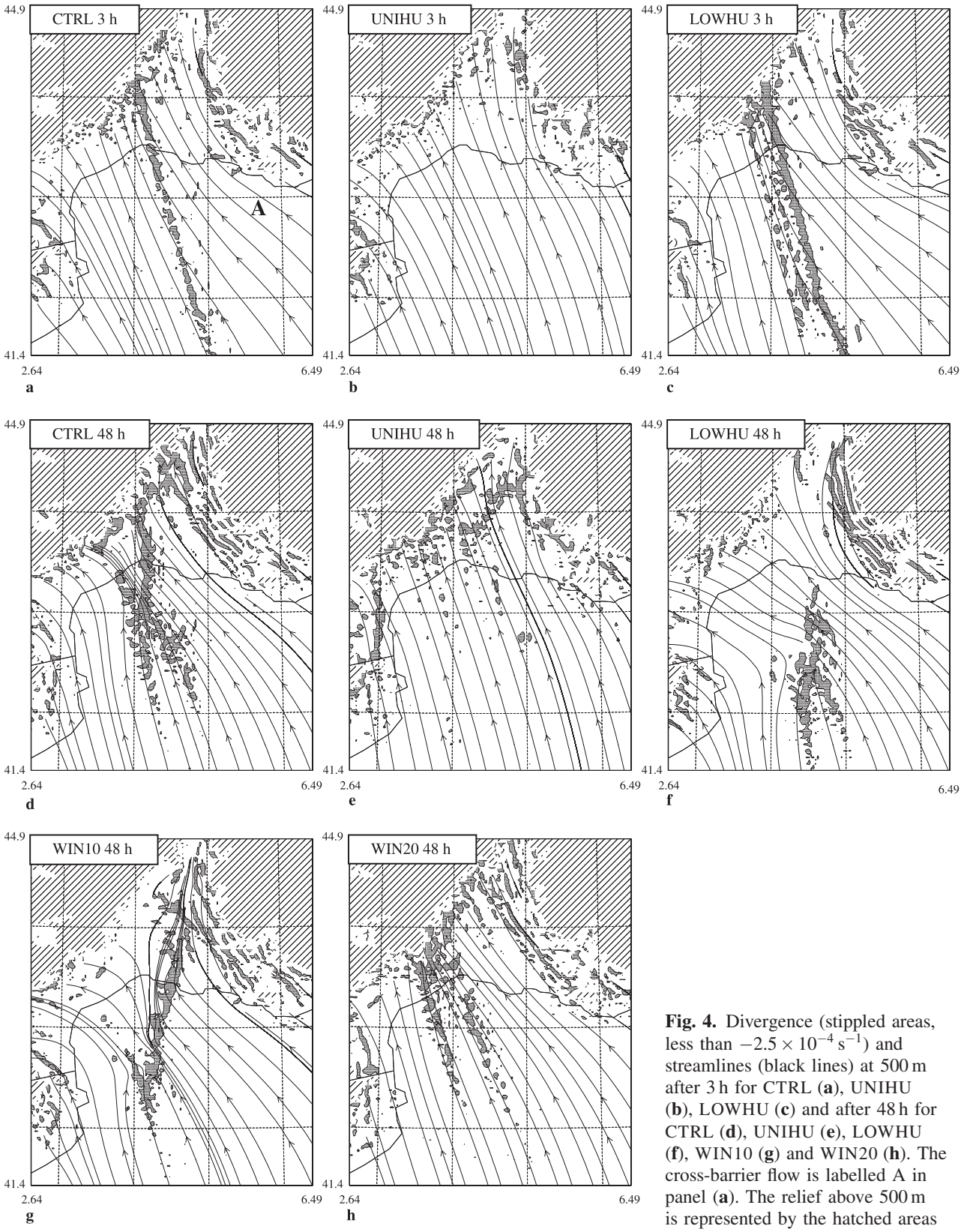

Fig. 4. Divergence (stippled areas, less than $-2.5 \times 10^{-4}\,s^{-1}$) and streamlines (black lines) at 500 m after 3 h for CTRL (**a**), UNIHU (**b**), LOWHU (**c**) and after 48 h for CTRL (**d**), UNIHU (**e**), LOWHU (**f**), WIN10 (**g**) and WIN20 (**h**). The cross-barrier flow is labelled A in panel (**a**). The relief above 500 m is represented by the hatched areas

With a uniform high humidity, the mesoscale convective system forms and stays over the relief of the Massif Central (Fig. 6a). Other precipitating cells are also triggered by the Pyrenees and the Alps. The main mechanism for triggering new convective cells at the same location is the

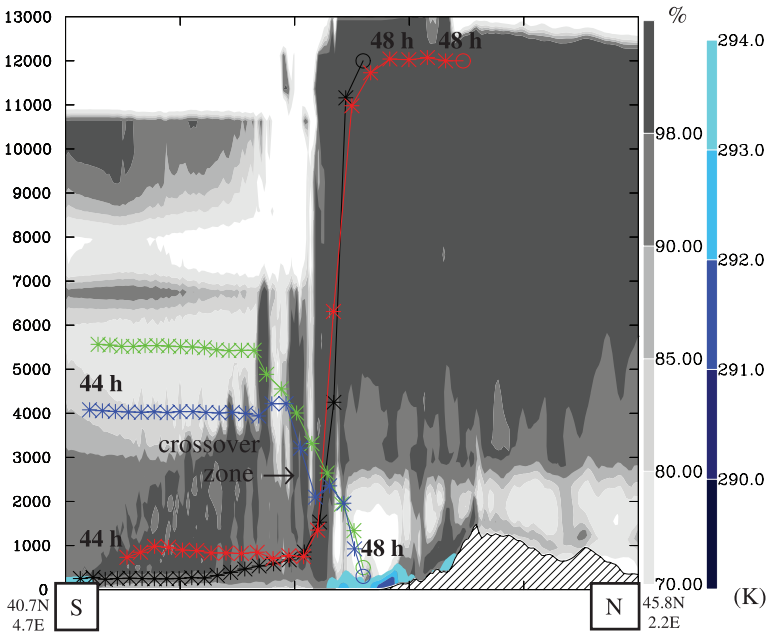

Fig. 5. Vertical cross-section along the line S–N shown in Fig. 2b of relative humidity (grey scale, %) and virtual potential temperatures (colour scale, K) for the simulation CTRL after 48 h. Some backward trajectories between 48 h and 44 h are also drawn

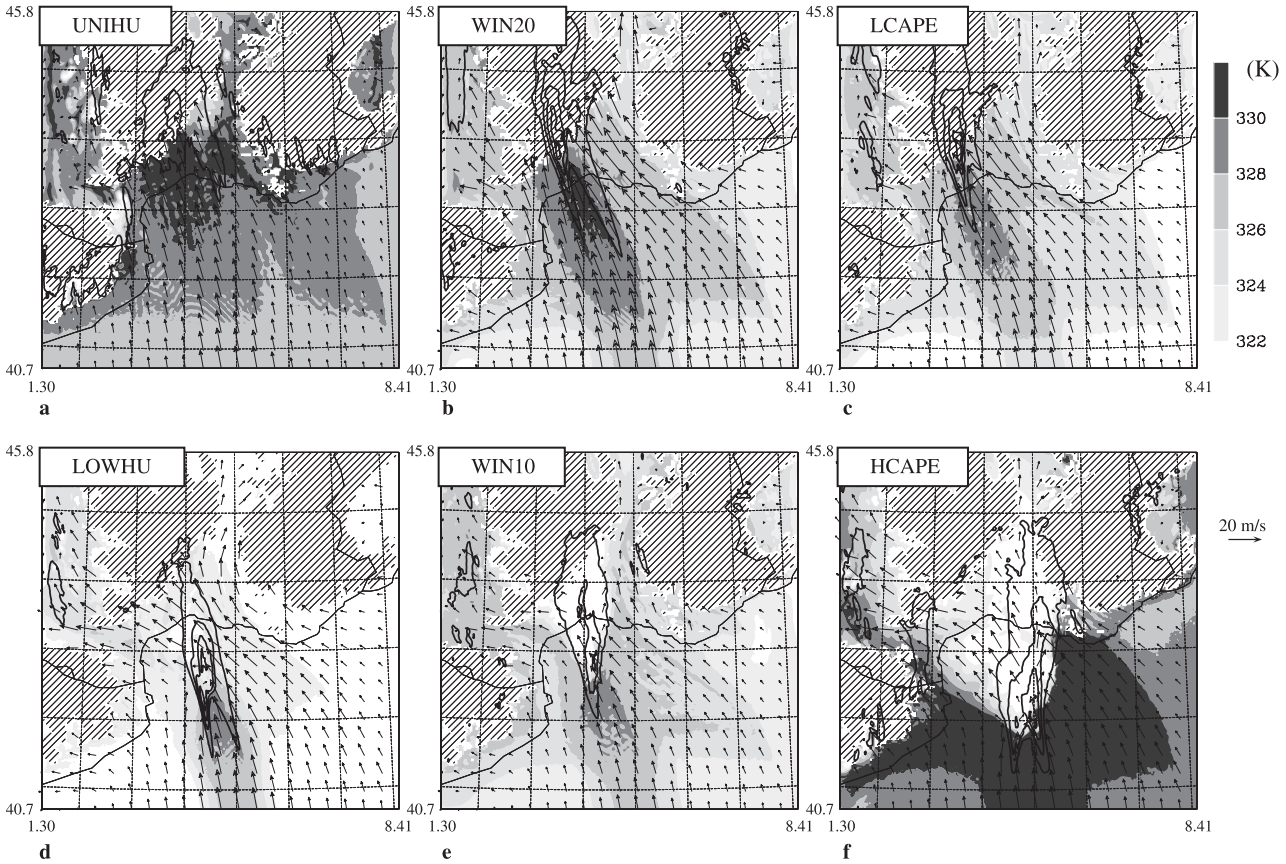

Fig. 6. Equivalent potential temperature at 500 m (grey scale, K), 500-m ASL wind vectors (black arrows, m/s) and 24-h accumulated precipitation (black lines, 50, 100, 250, 500 and 750 mm) after 48 h for simulations UNIHU (**a**), WIN20 (**b**), LCAPE (**c**), LOWHU (**d**), WIN10 (**e**) and HCAPE (**f**). The relief above 500 m is represented by the hatched areas

orographic lifting of the moist and unstable flow when it impinges the Massif Central. Indeed, a large part of the incoming flow is forced up when reaching the Massif Central southeastern slopes. Despite some punctual cooling beneath the precipitation (Fig. 3a), there is no well-developed

cold pool within this simulation as shown by Table 1 which displays the area of the surface with low-level temperature below 294.5 K and 292 K, respectively. Increasing the mixing ratio of water vapour outside of the jet favours the flow over the mountains in detriment of ‘‘flow around’’ as shown by Miglietta and Buzzi (2001). Indeed, the deflection of the flow by the Alps is considerably reduced in the simulation UNIHU and also therefore the upstream low-level convergence over the Sea (Fig. 4b, e).

Decreasing the mixing ratio of water vapour outside the jet in LOWHU leads to the formation of an intense cold pool (Table 1) which spreads southeastward over the Sea (Fig. 3d). The convective system is mainly located over the Sea (Fig. 6d) with a high maximum of precipitation (Table 1). The leftward deflection of drier air by the Alps is more accentuated compared to the CTRL run and accentuates the low-level convergence upwind of the Massif Central during the first hours of the simulation (Fig. 4c). Later, the low-level convergence is located more upstream as the cold pool extends farther over the Sea (Fig. 4f).

Figure 7 shows the vertical velocity averaged over the precipitating system for all simulations. Simulation LOWHU, as well as CTRL, produces larger upward vertical velocity within the convective system than UNIHU (Fig. 7a) for which the updrafts are more fragmented and less organized (Fig. 3a). When the distribution of humidity is high and uniform (UNIHU), there is no cold pool (Table 1) indicating that the evaporation of falling precipitation is reduced compared to CTRL and LOWHU ones as the environment is more humid in UNIHU. Downdrafts are thus weaker. Although the surface with precipitation is the largest in UNIHU (Table 1), the precipitation total and extent of the area with heavy precipitation (>200 mm) are smaller. It is worth noting that the precipitating system in UNIHU is less efficient because weaker precipitation totals are produced whereas the amount of available moisture is higher.

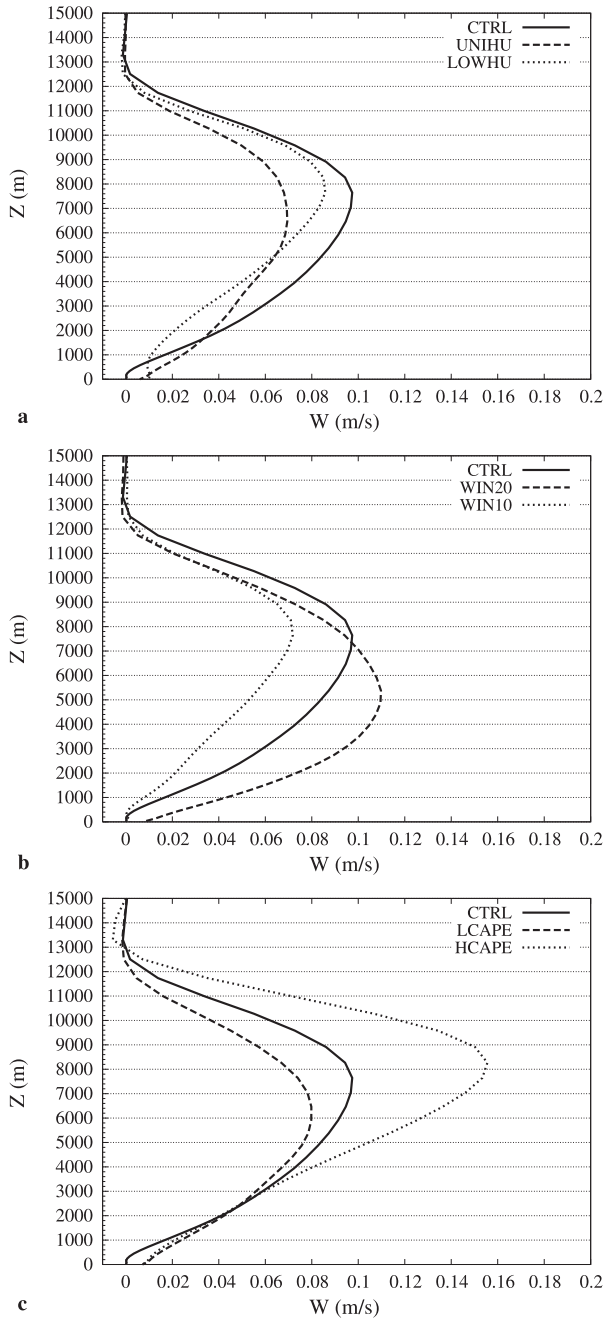

Fig. 7. Vertical velocities (m/s) averaged over the precipitating system (subdomain defined in Fig. 2c) for the different simulations after 48 h for simulations CTRL, UNIHU and LOWHU (**a**), for simulations CTRL, WIN10 and WIN20 (**b**), and for simulations CTRL, LCAPE and HCAPE (**c**)

3.3 Effect of the wind speed

Simulations WIN10 and WIN20 highlight the effect of the flow speed on the location and intensity of the quasi-stationary system. With a stronger flow (WIN20), the system is located over the relief (Fig. 6b), there is no cold pool (Fig. 3b, Table 1) and lifting is favoured by orography (Fig. 3b). Increasing the speed of the flow leads to favour ‘‘flow over’’ instead of ‘‘flow around’’. Therefore, there is less deflection of the flow by

the Alps in WIN20 (Fig. 4h). This result is in agreement with the Chu and Lin (2000) and Chen and Lin (2005) studies that showed that idealized moist flow regimes with large moist Froude numbers tend to generate quasi-stationary convective systems over their ideal mountain ridge or downstream-propagating convective systems.

In WIN10, as the flow is weaker, deflection by the Alps is favoured (Fig. 4g). The convective system is located upstream over the Sea (Fig. 6e) with a well-developed cold pool (Table 1). This cold pool contributes to enhance the low-level convergence over the Sea and over the Rhone valley. Upward forcing is located along the eastern leading edge of this strong cold pool (Fig. 3e). With weaker winds, the cold pool can interact with the incident flow whereas with larger winds, the rapid flow doesn't allow any cold pool to set-up.

Varying the wind speed acts to increase or decrease the moisture feeding of the convective system and thus modulates the precipitation totals. Moreover, the evaporation from the Sea contributes to increase the mixing ratio of water vapour in the low levels. This evaporative contribution is increased when the wind is intensified. Thus WIN20 produces a more intense low-level moisture flow with more precipitation totals whereas it is the opposite for WIN10 (Table 1). The mean vertical velocities over the convective system are stronger when the flow that feeds the system is stronger (Fig. 7b). Conversely, the stronger the flow is, the smaller the total precipitation area is. That can be explained by the difference between the lifting mechanisms involved in the formation and maintaining of the convective system. Indeed, in the case of a strong flow (WIN20), the main forcing is orographic lifting due to the Massif Central relief whereas for a weaker flow (WIN10), both the cold pool and the low-level convergence contribute to form repeatedly new cells along the eastern leading edge of the cold pool. The simulation CTRL appears as an intermediary solution where the three mechanisms are involved (cold pool dynamics, low-level convergence and orographic lifting).

3.4 Effect of the instability

Finally, CAPE has been varied in LCAPE and HCAPE experiments by modifying the low-level thermodynamic characteristics of the sounding used for initial and boundary conditions (Fig. 1a): the low-level temperature and mixing ratio are increased (decreased) to rise (or to reduce) the CAPE. The level of free convection of the initial sounding is therefore higher by 50 hPa in LCAPE and lower by 100 hPa in HCAPE compared to CTRL. The Downdraft Convective Available Potential Energy (DCAPE), which is a parameter used to estimate the potential strength of rain-cooled downdrafts, is also lowered in LCAPE by 5 J/kg and significantly increased by 120 J/kg in HCAPE.

When the CAPE is decreased, the convective system anchors over the relief (Fig. 6c), as in simulation WIN20 with a very weak cold pool (Fig. 3c, Table 1). Convective cells form both within the upstream low-level wind convergence area and over the relief. On the contrary, when increasing instability, a cold pool forms under the convective system (Fig. 3f). The simulation HCAPE (Fig. 6f) generates the strongest cold pool of all the simulations (Table 1) that spreads southeastward over the Sea and within the Rhone valley between the Massif Central and the Alps (Fig. 3f). Larger CAPE produces more intense updrafts (Fig. 7c) and more precipitating hydrometeors (not shown). Loading and evaporation of this larger amount of hydrometeors, in an environment with larger DCAPE, lead to more intense downdrafts (not shown) and cold pool, which in its turn reinforces the upward lifting at the leading edge of the convective system. The large subsidence areas under the precipitating system in Fig. 3f give an insight of the strength of these downdrafts. The boundary between the incident flow and this strong cold pool establishes more upstream in HCAPE than in the other simulations.

The precipitation totals and the area coverage of the precipitating system increase with the instability, which can be also attributed to the increase of the mixing ratio. The simulation HCAPE produces the largest precipitation amount (6.24 km^3, Table 1), although the highest maximum of precipitation is obtained for the simulation LCAPE. Indeed, as in simulation WIN20, the relief exerts a very local and stationary forcing that focuses the precipitation over a small zone. For these two experiments, the precipitating cells repeatedly form over the same limited area, whereas for HCAPE and WIN10

new cells trigger all along the leading edge of the cold pool that is wider and less stationary than the orographic forcing area.

4. Conclusion

In this study, idealized high-resolution simulations have been performed to study the sensitivity of the location and intensity of the precipitating systems with respect to the characteristics of the low-level flow over the Mediterranean Sea. Figure 8 provides a synthesis view of the results. Various lifting mechanisms are involved to explain the specific location of the heaviest precipitation (orographic lifting, cold pool dynamics, low-level convergence due to deflection of the flow by the Alps). Their respective importance depends on the characteristics of the flow. It is found that low-level moisture has an impact on the cold pool formation, the deflection of the flow by relief (''flow over'' or ''flow around'') and the location of the convective system. Sensitivity experiments show that:

- when the speed of the upstream flow is increased (decreased) compared to the CTRL run, the area of maximum precipitation moves downstream (upstream);
- when the mixing ratio of the environment outside of the jet is less (more) than in the CRTL run, the system is located more upstream (downstream);
- when the instability of the upstream flow is increased (decreased) compared to the CTRL run, the convective system moves upstream (downstream).

The cold pool strength increases with a slower flow and/or more instability. The maximum of rainfall is obtained when the convective system is over the relief with a strong low-level flow or a weak CAPE. The surface covered by heavy precipitation is maximum when CAPE is high or low-level flow is strong. However, it is worth mitigating the role of CAPE as when varying this parameter in the experiments, other parameters such as DCAPE and CIN are also modified in the experiments.

This study shows that the location and amount of precipitation associated with quasi-stationary convective systems over Mediterranean coast of southeastern France can not be only amounted to a problem of a flow over a mountain ridge (the Massif Central). Both the effects of the neighbouring mountains and the interaction with the convective system itself have to be considered. This makes the forecasting of the location and intensity of the heavy precipitation events complex as the interactions of the moist unstable flow with these competing or additional ingredients have to be taken into consideration.

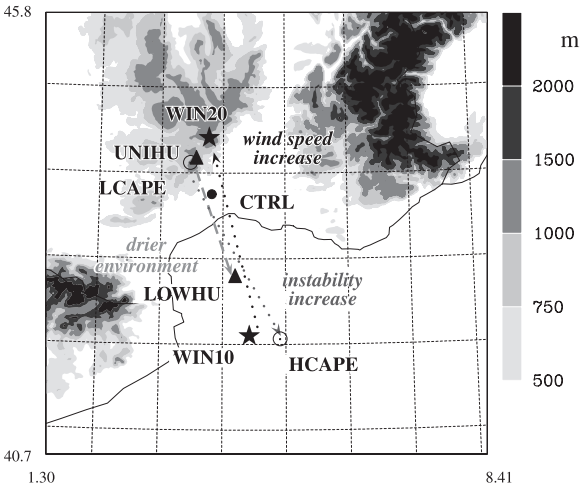

Fig. 8. Synthesis view of the location of 24-h heaviest precipitation areas for the different experiments (triangles for UNIHU and LOWHU, stars for WIN10 and WIN20, circles for LCAPE and HCAPE, bullet point for CTRL), the arrows indicate the ''displacement'' of the convective system when drying the environment (dashed grey arrow), when increasing the instability (dotted dark grey arrow) and when increasing the flow speed (dotted black arrow). The relief is represented in grey scale (m)

Acknowledgments

This study benefited from support from the national research program LEFE of the Institut National des Sciences de l'Univers through the VAPIMED project. We also thank our reviewers for very careful reading of the original typescript, which led to many improvements.

References

Chen S-H, Lin Y-L (2005) Orographic effects on a conditionally unstable flow over an idealized three-dimensional mesoscale mountain. Meteorol Atmos Phys 88: 1–21

Chu C-M, Lin Y-L (2000) Effects of orography on the generation and propagation of mesoscale convective systems in a two-dimensional conditionally unstable flow. J Atmos Sci 57: 3817–37

Davolio S, Buzzi A Malguzzi P (2006) Orographic influence on deep convection: case study and sensitivity experiments. Meteorologische Zeitschrift 15: 215–23

Delrieu G, Ducrocq V, Gaume E, Nicol J, Payrastre O, Yates E, Kirstetter P-E, Andrieu H, Ayral P-A, Bouvier C, Creutin J-D, Livet M, Anquetin S, Lang M, Neppel L, Obled C, Parent du Châtelet J, Saulnier G-M, Walpersdorf A, Wobrock W (2005) The catastrophic flash-flood event of 89 September 2002 in the Gard region, France: a first case study for the Cévennes-Vivarais Mediterranean Hydrometeorological Observatory. J Hydrometeor 6: 34–52

Ducrocq V, Nuissier O, Ricard D, Lebeaupin C, Thouvenin T (2008) A numerical study of three catastrophic precipitating events over western Mediterranean region (southern France). Part II: Mesoscale triggering and stationarity factors. Quart J Roy Meteor Soc 34: 131–45

Gheusi F, Stein J (2003) Small-scale rainfall mechanisms for an idealized convective southerly flow over the Alps. Quart J Roy Meteor Soc 129: 1819–40

Lafore J-P, Stein J, Asencio N, Bougeault P, Ducrocq V, Duron J, Fischer C, Héreil P, Mascart P, Masson V, Pinty J-P, Redelsperger J-L, Richard E, Vilà-Guerau de Arellano J (1998) The Meso-NH atmospheric simulation system. Part I: Adiabatic formulation and control simulations. Scientific objectives and experimental design. Ann Geophys 16: 90–109

Lin Y-L, Chiao S, Wang T-A, Kaplan ML, Weglarz RP (2001) Some common ingredients for heavy orographic rainfall. Wea Forecast 16: 633–60

Miglietta MM, Buzzi A (2001) A numerical study of moist stratified flows over isolated topography. Tellus A 53: 481–99

Nuissier O, Ducrocq V, Ricard D, Lebeaupin C, Anquetin S (2008) A numerical study of three catastrophic precipitating events over western Mediterranean region (Southern France). Part I: Numerical framework and synoptic ingredients. Quart J Roy Meteor Soc 134: 111–30

Ricard D (2005) Modélisation à haute résolution des pluies intenses dans les Cévennes: Le système convectif des 13 et 14 octobre 1995. La Météorologie 8e série 48: 28–38

Rotunno R, Ferretti R (2001) Mechanisms of intense Alpine rainfall. J Atmos Sci 58: 1732–49

Rotunno R, Klemp JB, Weisman ML (1988) A theory for strong, long-lived squall lines. J Atmos Sci 45: 463–85

Schumacher RS, Johnson RH (2005) Organization and environmental properties of extreme-rain-producing mesoscale convective systems. Mon Wea Rev 133: 961–76